Catalytic reduction of NO on copper/MCM-41 studied by in situ EXAFS and XANES

Y.-J. Huang [a], H. Paul Wang [b,*], Jyh-Fu Lee [c]

[a] *Department of Environmental and Safety Engineering, Chung Hwa College of Medical Technology, Tainan 717, Taiwan*
[b] *Department of Environmental Engineering, National Cheng Kung University, 1 University Road, Tainan 70101, Taiwan*
[c] *Synchrotron Radiation Research Center, Hsinchu 300, Taiwan*

Abstract

Speciation of copper in the channels of MCM-41 during reduction of NO with CO at 473–773 K was studied by in situ extended X-ray absorption fine structural (EXAFS) and X-ray absorption near edge structural (XANES) spectroscopies in the present work. The component fitted (in situ) XANES spectra of the catalyst showed that about 72% of metallic copper (Cu(0)) in MCM-41 was oxidized to higher oxidation state coppers (Cu(II) (46%) and Cu(I) (26%)) during the NO reduction process (at 473 K). By EXAFS, we also found that in the NO reduction process, oxygen was inserted into the metallic copper matrix and led to a formation of the copper oxide species with a Cu–O bond distance of 1.93 Å which was greater than that of the model compound Cu_2O (typically 1.86 Å). At 573–673 K, mainly Cu(II) was found in the channels of MCM-41. Nevertheless, at a higher temperature (e.g., 773 K), about 61% Cu(I), 31% Cu(II), and 8% Cu(O) with averaged Cu–Cu and Cu–O bond distances of 3.04 and 1.88 Å, respectively were observed, that might account for the high selectivity-to-decomposition (S/D) ratios for yields of N_2 and CO_2 in the catalytic reduction of NO with CO.
© 2002 Elsevier Science Ltd. All rights reserved.

Keywords: NO reduction; Cu/MCM-41; XANES; EXAFS

1. Introduction

Nitrogen oxides (NO_x) may cause photochemical smog formation, acid rain, atmospheric visibility degradation and adverse effects on human health. About 3×10^7 tons per year of NO_x are vented to the atmosphere (Armor, 1995). Reduction of NO_x is, therefore, one of the most important issues in the air pollution control and environmental protection. Methods such as reduction–absorption, chelation absorption, and cata-lytic decomposition and reduction for reduction of NO_x in the emission control processes have been widely studied (Li and Hall, 1991; Iwamoto et al., 1993; Perlmutter et al., 1993). NO can be catalytically reduced with CO, hydrocarbons or H_2 (Mergler et al., 1995). Reduction of NO with H_2 can proceed at a lower temperature than that with CO. Since CO is frequently found in ineffective combustion or incineration processes, the concentration of CO in the exhaust gas is generally greater than that of H_2 by about 10 times (Mergler et al., 1995).

Iwamoto et al. (1993) have demonstrated that Cu-exchanged zeolites, particularly Cu/ZSM-5, are very effective in catalytic reduction of NO. However, reduction of NO on Cu/ZSM-5 may be inhibited by O_2 and H_2O and readily poisoned by SO_2 (Misono et al., 1997). Due to a diffusion restriction of NO caused by the active

copper species in the confined channels (5.5–6.0 Å) of ZSM-5, catalytic reduction of NO on Cu/ZSM-5 was, to some extent, not very effective (Misono et al., 1997). Mobil's composition of matter 41 (MCM-41) has a hexagonal arrangement of uni-dimensional mesopores with diameters of 15–100 Å (Beck et al., 1992; Kresge et al., 1992). In addition, MCM-41 is thermally stable at 1300 K with high surface areas of 500–1500 m^2/g (Corma et al., 1995). MCM-41, in fact, bridges the gap between microporous zeolites and macroporous amorphous aluminosilicates for catalysis and separation engineering.

Extended X-ray absorption fine structural (EXAFS) and X-ray absorption near edge structural (XANES) spectroscopies are very useful in determination of elements with a different environment and degree of aggregation or location (Burch and Scire, 1994; Huang and Wang, 1999; Palomino et al., 2000). In situ EXAFS and XANES can observe the catalytic process directly from the perspective of the active site during reactions. X-rays can penetrate into the catalyst at reaction temperatures and pressures while monitoring the electronic and local structure of the catalytically active elements. Thus, the main objective of the present work was to study the speciation of copper in the channels of MCM-41 in the catalytic NO reduction process by in situ EXAFS and XANES spectroscopies.

2. Experimental

In the MCM-41 synthesis process, a mixture containing sodium silicate solution (14 wt.% NaOH, and 27 wt.% SiO_2) (Fisher Scientific), fumed silica (Sigma), cetyltrimethylammonium bromide (CTMABr) gel (TCI-EP) and tetramethylammonium hydroxide (TMAOH) (Lancaster) was stirred well at 298 K for 2 h. The molar ratio of the mixture was SiO_2:TMAOH:CTMABr:H_2O = 1.0:0.27:0.58:86. A diluted sulfuric acid solution was used to adjust the pH values of the mixture solution between 11 and 12. The mixture was then heated in a teflon lined autoclave (100 ml) at 423 K for 48 h. The as-synthesized MCM-41 was filtered, washed with deionized water, dried at 378 K for 16 h and calcined at 823 K for 10 h. The Cu/MCM-41 (5 wt.%) catalyst was prepared by impregnation of an aqueous solution of 0.1 M $Cu(NO_3)_2$ (Merck) onto the MCM-41. The catalyst was dried at 378 K for 16 h and calcined at 823 K for 2 h. Structure of the catalyst was characterized by X-ray powder diffraction spectroscopy (RIGAKU, Model D/MAX III–V).

Catalysts were reduced in a flowing 10% H_2/He (30 ml/min) gas at 573 K for 1 h. About 1.0 g of the catalyst was used in the catalytic reduction of NO (2% NO and 2% CO balanced by He) in a home-made in situ EXAFS cell. Composition of the product gases was determined by on-line FTIR and GC (with a column of molecular sieve 5A). Infrared spectra were recorded on a FTIR spectrometer (Digilab (FTS-40)) with fully computerized data storage and data handling capability. For all spectra reported, a 64-scan data accumulation was carried out at a resolution of 4 cm^{-1}.

EXAFS and XANES spectra were recorded on the Wiggler beamline at the Taiwan SRRC. The electron storage ring was operated at energy of 1.5 GeV (ring current = 120–200 mA). A Si(1 1 1) double-crystal monochromator was used for selection of energy. The energy resolution $\Delta E/E$ of the beamline was about 1.9×10^{-4} (eV/eV). EXAFS spectra were measured in the transmission mode. Photon energy was calibrated by characteristic preedge peaks in the absorption spectrum of a Cu foil (8979 eV). The standard deviation calculated from the averaged spectra was used to estimate the statistical noise and error associated with each structural parameter. The EXAFS data were analyzed using the UWXAFS 3.0 and FEFF 8.0 programs (Stern et al., 1995). The isolated EXAFS spectra were normalized to the edge jump, converted to the wavenumber scale and Fourier transformed on k^3-weighted EXAFS oscillations in the range of 2.8–14 $Å^{-1}$.

The absorption edge was determined at the half-high (precisely determined by the derivative) of the XANES spectrum after preedge baseline subtraction and normalization to the maximum postedge intensity. Principal component (factor) analysis was used in the data treatment to optimize the quantitative extraction of relative concentrations. XANES spectra of model compounds such as CuO, Cu_2O, and Cu foil were also measured on the Wiggler beamline. On the average, an uncertainty limit of 5% corresponds to an error of $\approx 2.0\%$ in the fitting results. Semi-quantitative analyses of the edge spectra were conducted by the least-square fitting of linear combinations of standard spectra to the spectrum of the sample. The height and area of the near edge band in a copper spectrum were quantitatively proportional to the amount of copper species.

3. Results and discussion

Fig. 1 shows the X-ray diffraction (XRD) pattern of the CuO/MCM-41 catalyst. At low diffraction angles (2θ), the well-defined peaks at (1 0 0), (1 1 0), (2 0 0) and (2 1 0) were suggestive of a hexagonal mesopore system for the MCM-41 (Wu and Bein, 1996). Note that the wall of the MCM-41 was in an amorphous state. The (1 0 0) peak can be indexed on a hexagonal lattice with a pore diameter of about 45 Å. The structural parameters (d_{100} spacing, the unit cell parameter ($a_0 = 2d_{100}/\sqrt{3}$), average pore diameter, and surface area) of the MCM-41 are also listed in the upper corner of Fig. 1. By XRD, we found that impregnation of copper into hexagonal
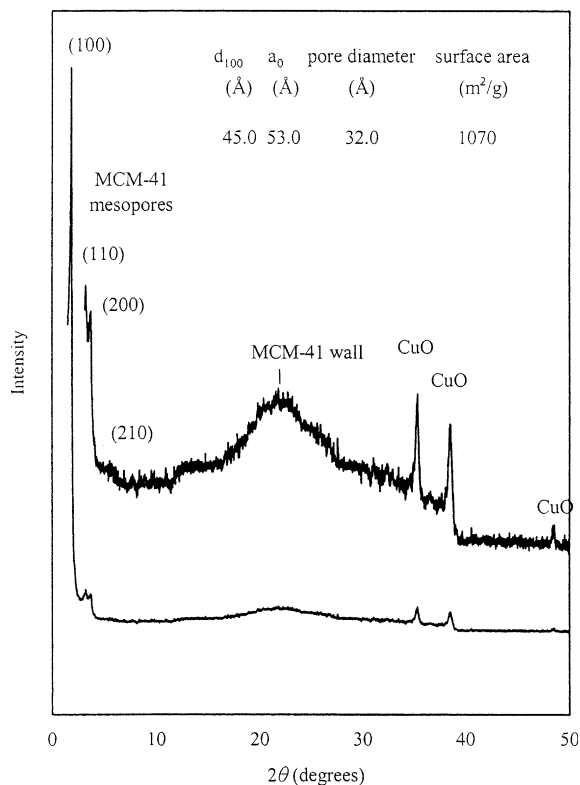
Fig. 1. XRD pattern of the Cu/MCM-41 catalyst. Structural parameters of the catalyst are also shown in the upper corner.
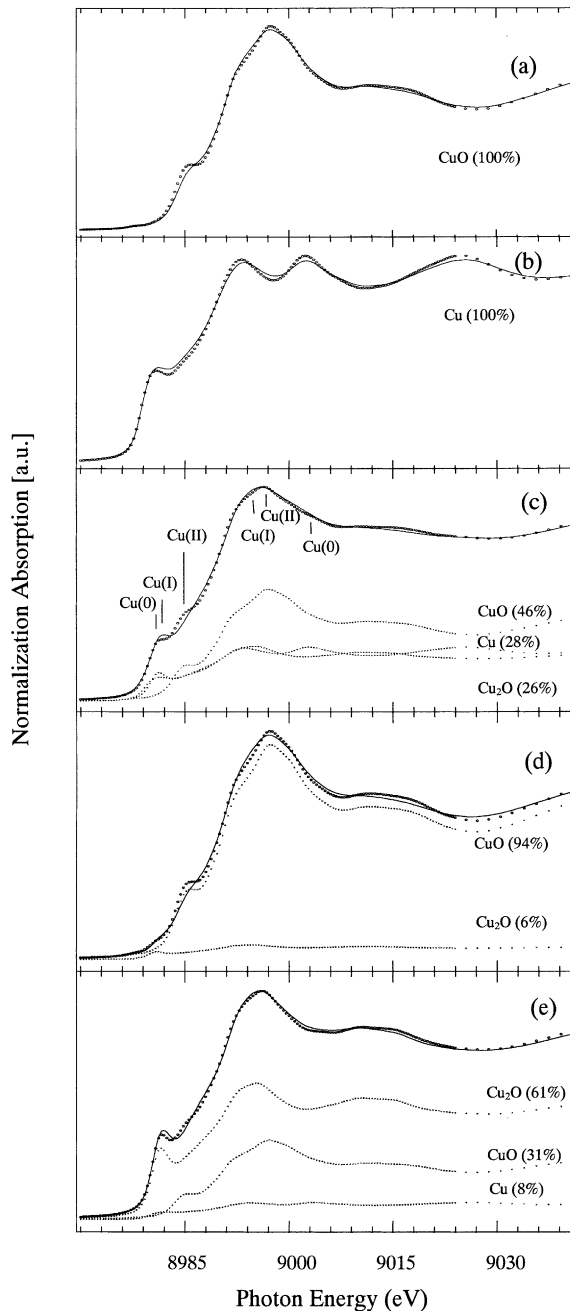

Fig. 2. In situ XANES spectra of (a) oxidized Cu/MCM-41, (b) reduced Cu/MCM-41, and the reduced Cu/MCM-41 catalyst involved in reduction of NO with CO at (c) 473 K, (d) 573 K and (e) 773 K.

pores of MCM-41 caused little perturbation on the MCM-41 framework. Mainly copper oxides were found in MCM-41.

In order to investigate the speciation of copper that involved in the catalytic reduction of NO with CO, in situ EXAFS and XANES spectra of the catalyst were also measured at 473–773 K under reaction conditions. These XANES curves were best fitted with spectra of model compounds such as Cu, Cu_2O and CuO. In Fig. 2(a), the preedge XANES spectra (8975–8979 eV) of the oxidized Cu/MCM-41 catalyst exhibit a very weak 1s-to-3d transition forbidden by the selection rule in the case of the perfect octahedral symmetry. A shoulder at 8985–8988 eV and an intense band at 8994–9002 eV can be attributed to the 1s-to-4p transition that indicates the existence of the Cu(II) species. The XANES spectrum of the reduced Cu/MCM-41 catalyst (Fig. 2(b)) was very similar to that of the Cu foil. It should be noted that the metallic copper Cu(0) has a very low activity in NO reduction generally (Kharas et al., 1993).

The in situ XANES spectrum for catalytic reduction of NO with CO on Cu/MCM-41 at 473 K is shown in Fig. 2(c). The preedge band at 8981–8984 eV might be attributed to the dipole-allowed 1s-to-4p transition of Cu(I) that was formed via oxidation of Cu(0) with NO.

The component fits of the XANES spectra showed that approximately 72% of Cu(0) were oxidized to Cu(I) (26%) and Cu(II) (46%) species during the NO reduction process at 473 K (see Fig. 2(b)). Generally, Cu(I) species is very active in catalytic reduction of NO (Spoto et al.,

1994; Konduru et al., 2001). Liu and Robota (1994) found that the Cu(I) species corresponded to the reduction of NO to N_2 in the presence of propene at 500–700 K.

In Fig. 3, the S/D ratios (selectivity-to-decomposition = yield of N_2/disappearance of NO) for N_2 yield increased as the reaction temperature increased (at 473–773 K). N_2O was formed via a surface reaction between surface species $NO_{(ad)}$ and $N_{(ad)}$ ($NO_{(ad)} + N_{(ad)} \leftrightarrow N_2O_{(g)}$). Since heat of adsorption for oxygen atoms on the copper surface is −79 kcal/mol which is less than the heat of formation for $1/2$ O_2 (−69.9 kcal/mol) (Yokomichi and Yamabe, 1996), oxygen molecules might not be formed on the copper surfaces at temperatures less than 673 K.

Based on the gas phase nitrogen and oxygen (NO, N_2O, NO_2, CO, CO_2, and O_2) balance calculations (Konduru et al., 2001; Treesukol et al., 2001), we found that about 7% of total oxygen atoms yielded from the dissociative NO adsorption ($NO \rightarrow N_{(ad)} + O_{(ad)}$) were consumed in the yields of N_2O and CO_2 in the NO reduction process. Most oxygen (93%) might involve in

the oxidation of the metallic copper (Cu(0)) to Cu(I) and Cu(II) species. Interestingly, the XANES absorbance at 8981–8984 eV for the Cu(I) species, to some extent, was decreased possibly due to oxidation of Cu(I) to Cu(II) in the NO reduction process at 573 K (see Fig. 2(d)). At 773 K, fractions of Cu(I) and Cu(0) in MCM-41 were increased during the NO reduction process (Fig. 2(e)). An enhancement on decomposition of NO to N_2 was, therefore, observed in Fig. 3(b).

In order to further understand the speciation of copper in MCM-41, in situ EXAFS spectra of the catalyst were also determined. Fig. 4 shows the EXAFS data of copper in the catalysts and their fits in r-space of the radial structural functions. The oxidized Cu/MCM-41 has a Cu–O bond distance of 1.96 Å with a CN of 3.3 (Table 1). In the second shells, the Cu–(O)–Cu bond distance and CN were 2.97 and 5.7 Å, respectively. Reduction of the catalyst in hydrogen at 573 K led to a formation of Cu–Cu species with a bond distance of 2.54 Å. The CN of the Cu–Cu species in the channels of MCM-41 was 9.0. Reduction of NO with CO on the reduced Cu/MCM-41 catalyst at 473 K caused the oxi-
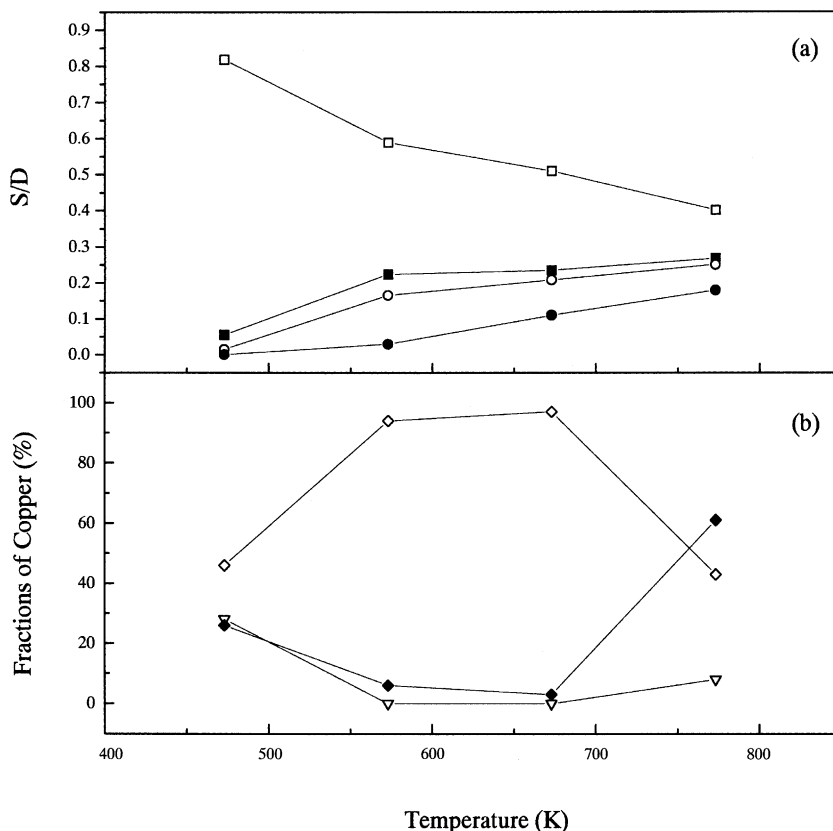

Fig. 3. Temperature dependence for (a) S/D (selectivity-to-decomposition ratios) of NO (□), N_2O (■), CO_2 (○), and N_2 (●) for catalytic reduction of NO with CO on Cu/MCM-41 and (b) fraction (%) of Cu(0) (▽), Cu(I) (◆) and Cu(II) (◇) in MCM-41.
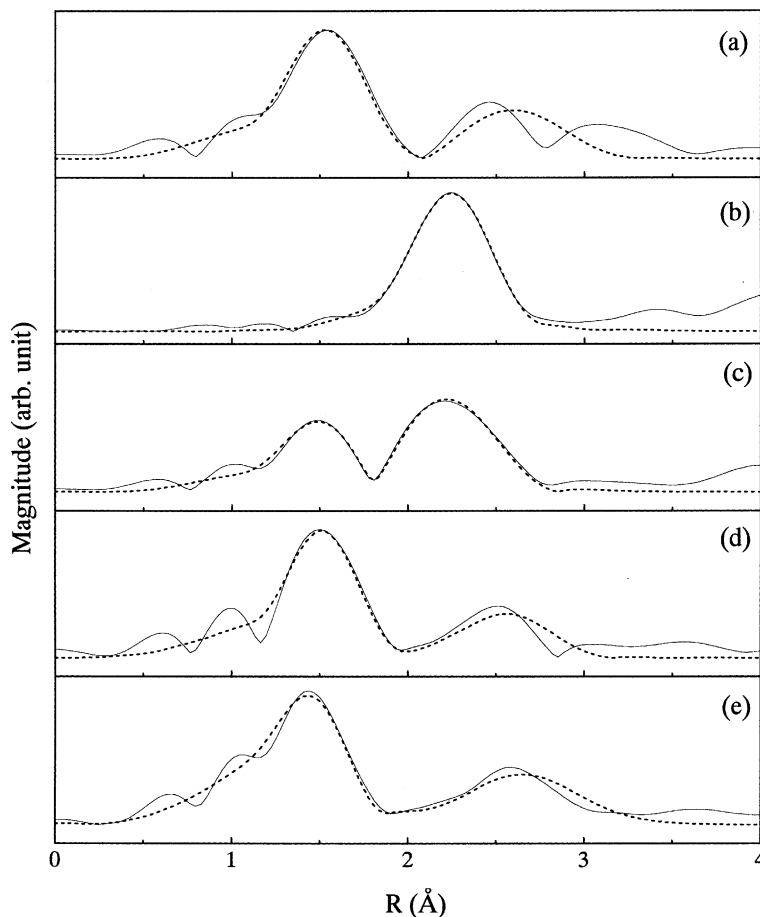
Fig. 4. Fourier transformed Cu K-edge EXAFS of (a) oxidized Cu/MCM-41, (b) reduced Cu/MCM-41, and the reduced Cu/MCM-41 catalysts for reduction of NO with CO at (c) 473 K, (d) 573 K and (e) 773 K. The dotted curves denote the best fitting of the EXAFS spectra.

Table 1
Speciation parameters of the Cu/MCM-41 catalysts

Catalyst	Shells	Bond distance (Å)	Coordination number	σ^2 (Å^2)
Oxidized Cu/MCM-41	Cu–O	1.96	3.3	0.0044
	Cu–(O)–Cu	2.97	5.7	0.0208
Reduced Cu/MCM-41	Cu–Cu	2.54	9.0	0.0089
Cu/MCM-41[a]	Cu–O	1.93	2.0	0.0066
	Cu–Cu	2.58	1.9	0.0076
Cu/MCM-41[b]	Cu–O	1.94	2.5	0.0028
	Cu–(O)–Cu	2.93	1.3	0.0068
Cu/MCM-41[c]	Cu–O	1.88	2.0	0.0050
	Cu–(O)–Cu	3.04	6.0	0.0248

σ: Debye–Waller factor.
Reduction of NO with CO on Cu/MCM-41 at (a) 473 K, (b) 573 K and (c) 773 K.

dation of the metallic copper (Cu(0)) to Cu(I) and Cu(II) as shown in the XANES spectrum in Fig. 2(c). The EXAFS spectra of the catalyst indicated that a mixture of the Cu(0), Cu(I) and Cu(II) species involved in the reduction of NO in MCM-41 at 473 K. The copper (Cu(II)) was coordinated with 2.1 oxygen atoms with a

Cu–O bond distance of 1.93 Å that was between those of model compounds Cu_2O (typically 1.86 Å) and CuO (typically 1.96 Å). Interestingly, in Fig. 4(c), insertion of oxygen atoms into the metallic copper (Cu–Cu bond distance = 2.54 Å in the second shells) in the NO reduction process may cause the Cu–Cu bond distance to be slightly increased by 0.04 Å, that also led to the formation of a very active site (Cu(I)) for reduction of NO. By XANES, we also found that 26% of the metallic copper were oxided to Cu(I) in the NO reduction process at 473 K.

At 573 K, most copper species was oxidized to Cu(II). Insertion of oxygen into the copper matrix in the channels of MCM-41 led to formations of Cu–O and Cu–(O)–Cu species possessing bonding distances of 1.94 and 2.93 Å, respectively. At 773 K, a self-reduction of Cu(II) to Cu(I) might occur (Kuroda et al., 1999). Copper in the catalyst is consisted of 61% Cu(I), 31% Cu(II) and 8% Cu(0). The averaged Cu–O and Cu–(O)–Cu bond distances were 1.88 and 3.04 Å, respectively.

4. Conclusions

By in situ XANES and EXAFS spectroscopies, we found that oxidation of the Cu(0) to Cu(I) (26%) and Cu(II) (46%) occurred at 473 K in the catalytic NO reduction process. The Cu–O bond distance (1.93 Å) of the active copper species was between the model compounds Cu_2O (typically 1.86 Å) and CuO (1.96 Å), suggesting an insertion of oxygen into the metallic copper matrix during the reduction of NO with CO. At 773 K, 61% Cu(I), 8% Cu(0) and 31% Cu(II) with averaged Cu–Cu and Cu–O bond distances of 3.04 and 1.88 Å, respectively was observed. The relatively high fraction of Cu(I) in MCM-41 might account for the high S/D ratios for yields of N_2 and CO_2 from the catalytic reduction of NO with CO.

Acknowledgements

References

Armor, J.N., 1995. Catalytic reduction of nitrogen-oxides with methane in the presence of excess oxygen—a review. Catal. Today 26 (2), 147–158.

Beck, J.S., Vartuli, J.C., Roth, W.J., Leonowicz, M.E., Kresge, C.T., Schmitt, K.D., Chu, C.T.W., Olson, D.H., Sheppard, E.W., Mccullen, S.B., Higgins, J.B., Schlenker, J.L., 1992. A new family of mesoporous molecular-sieves prepared with liquid-crystal templates. J. Am. Chem. Soc. 114 (27), 10834–10843.

Burch, R., Scire, S., 1994. Selective catalytic reduction of nitric-oxide with ethane and methane on some metal exchanged ZSM-5 zeolites. Appl. Catal. B 3 (4), 295–318.

Corma, A., Martinez, A., Martinezsoria, V., Monton, J.B., 1995. Hydrocracking of vacuum gas–oil on the novel mesoporous MCM-41 aluminosilicate catalyst. J. Catal. 153 (1), 25–31.

Huang, Y.J., Wang, H.P., 1999. Reduction of NO with CH_4 effected by copper-oxide clusters in the channels of ZSM-5. J. Phys. Chem. A 103 (33), 6514–6516.

Iwamoto, M., Mizuno, N., Yahiro, H., Taylor, K., Blanco, C.J., Nam, I.S., Bartholomew, C.H., Metcalfe, I.S., Iglesia, E., Sinev, M., Duprez, D., Armor, J., Misono, M., 1993. Selective catalytic reduction of NO by hydrocarbons in oxidizing atmosphere. Stud. Surf. Sci. Catal. 75, 1285–1298.

Kharas, K.C.C., Robota, H.J., Liu, D.J., 1993. Deactivation in Cu-ZSM-5 lean-burn catalysts. Appl. Catal. B 2, 225–237.

Konduru, M.V., Chuang, S.S.C., Kang, X., 2001. Probing the reactivity of adsorbed NO species by the CO and H_2 pulse during NO decomposition on Cu-ZSM-5. J. Phys. Chem. B 105 (44), 10918–10926.

Kresge, C.T., Leonowicz, M.E., Roth, W.J., Vartuli, J.C., Beck, J.S., 1992. Ordered mesoporous molecular-sieves synthesized by a liquid-crystal template mechanism. Nature 359 (6397), 710–712.

Kuroda, Y., Kumashiro, R., Yoshimoto, T., Nagao, M., 1999. Characterization of active sites on copper ion-exchanged ZSM-5-type zeolite for NO decomposition reaction. Chem. Phys. 1, 649–656.

Li, Y.J., Hall, W.K., 1991. Catalytic decomposition of nitric-oxide over Cu-zeolites. J. Catal. 129 (1), 202–215.

Liu, D.J., Robota, H.J., 1994. In-situ characterization of Cu-ZSM-5 by X-ray-absorption spectroscopy—XANES study of the copper oxidation-state during selective catalytic reduction of nitric-oxide by hydrocarbons. Appl. Catal. B 4 (2–3), 155–165.

Mergler, Y.J., Vanaalst, A., Nieuwenhuys, B.E., 1995. NO reduction by CO and H_2 over a Pt–CoO_x–SiO_2 catalyst—effect of CoO_x on activity and selectivity. ACS Symp. Ser. 587, 196–207.

Misono, M., Hirao, Y., Yokoyama, C., 1997. Reduction of nitrogen-oxides with hydrocarbons catalyzed by bifunctional catalysts. Catal. Today 38 (2), 157–162.

Palomino, G.T., Bordiga, S., Zecchina, A., Marra, G.L., Lamberti, C., 2000. XRD, XAS, and IR characterization of copper-exchanged Y zeolite. J. Phys. Chem. B 104 (36), 8641–8651.

Perlmutter, H.D., Ao, H.H., Shaw, H., 1993. Absorption of NO promoted by strong oxidizing-agents—organic tertiary hydroperoxides in n-hexadecane. Environ. Sci. Technol. 27 (1), 128–133.

Spoto, G., Zecchina, A., Bordiga, A., Ricchiardi, G., Martra, G., Leofanti, G., Petrini, G., 1994. Cu(I)-ZSM-5 zeolites prepared by reaction of H-ZSM-5 with gaseous CuCl—spectroscopic characterization and reactivity towards

carbon-monoxide and nitric-oxide. Appl. Catal. B 3 (2–3), 151–172.

Stern, E.A., Newville, M., Ravel, B., Yacoby, T., Haskel, D., 1995. The UWXAFS analysis package—philosophy and details. Physica B 209 (1–4), 117–120.

Treesukol, P., Limtrakul, J., Truong, T.N., 2001. Adsorption of nitrogen monoxide and carbon monoxide on copper-exchanged ZSM-5: a cluster and embedded cluster study. J. Phys. Chem. B 105 (12), 2421–2428.

Wu, C.G., Bein, T., 1996. Microwave synthesis of molecular-sieve MCM-41. Chem. Commun. (8), 925–926.

Yokomichi, Y., Yamabe, T., 1996. Theoretical-study of NO decomposition on Cu-ZSM-5 catalyst models using the density-functional method. J. Phys. Chem. 100 (34), 14424–14429.